MNE 23 (2024) 100256

Contents lists available at ScienceDirect

Micro and Nano Engineering

journal homepage: www.sciencedirect.com/journal/micro-and-nano-engineering

CVD graphene-MoS_2 Van der Waals heterostructures on the millimeter-scale

Nico Rademacher [a,b], Eros Reato [a], Lukas Völkel [a], Annika Grundmann [c], Michael Heuken [c,d], Holger Kalisch [c], Andrei Vescan [c], Alwin Daus [a,e,*], Max C. Lemme [a,b,*]

[a] Chair of Electronic Devices, RWTH Aachen University, 52074 Aachen, Germany
[b] AMO GmbH, Advanced Microelectronic Center Aachen, 52074 Aachen, Germany
[c] Compound Semiconductor Technology, RWTH Aachen University, 52074 Aachen, Germany
[d] AIXTRON SE, 52134 Herzogenrath, Germany
[e] Sensors Laboratory, Department of Microsystems Engineering, University of Freiburg, 79110 Freiburg, Germany

ARTICLE INFO

Keywords:
Van der Waals heterostructure
Graphene
MoS_2
Raman spectroscopy
Wet transfer

ABSTRACT

This study investigates the interactions between chemical vapor-deposited graphene and metal-organic chemical vapor-deposited molybdenum disulfide (MoS_2) in heterostructures assembled via wet transfer. We use Raman spectroscopy to quantitatively determine close coupling between graphene and MoS_2 based on the peak separations in graphene. Although annealing seems to be necessary after transfer to establish a close coupling, its parameters do not have a significant impact on the quality of coupling (for 100 °C $< T <$ 400 °C and 5 min $< t <$ 120 min). Furthermore, the method is robust against variations in graphene thickness because bilayers can be distinguished by comparing the full width at half maximum of the graphene 2D peak. We expand our study to mm^2-scale areas of graphene-MoS_2 heterostructures finding that films assembled via wet-transfer technique exhibit considerable variability in terms of coupling strength. Evaluating such interactions in heterostructures on large areas is important for future practical applications in heterostructure devices.

1. Introduction

Van der Waals (VdW) heterostructures have gained broad interest in the fields of electronics [1], optoelectronics [2], nanoelectromechanical systems (NEMS) [3], and solid-state physics, e.g. in twist-angle heterostructures [4]. VdW heterostructures allow tuning the semiconductor conductivity type [5,6], bandgap [6–9], transistor on/off ratios [1,10], and photoluminescence [1]. In principle, this enables the engineering of heterostructures for many specific application scenarios. However, the strength of coupling between 2D materials in VdW heterostructures (hereafter referred to as heterostructures) strongly influences the properties of the resulting material stack. Measuring the interaction of the 2D materials in a non-destructive way, ideally over large areas, is therefore an important aspect for material development. Raman spectroscopy is well suited to accomplish this task [2,11–13], but studies are mostly limited to heterostructures of small flakes. The industrial implementation of heterostructure devices requires their fabrication and evaluation over large areas, which provides a measure of device variability and layer/heterostructure uniformity.

Here, we demonstrate Raman-based metrology of graphene and molybdenum disulfide (MoS_2) heterostructures that are assembled by wet transfer from large-area films grown by scalable (metal-organic) chemical vapor deposition (CVD) methods. We perform statistical analyses of Raman spectra for heterostructures up to the mm^2-scale and quantitatively evaluate the coupling between the two materials. Our results highlight variations in heterostructure coupling that need to be addressed for future application scenarios.

2. Materials and methods

We fabricated a structure in which graphene, MoS_2, and their heterostructures can be measured in close proximity to collect comparable Raman data for statistical analysis. Graphene was grown on copper by chemical vapor deposition (CVD), whereas MoS_2 was deposited on sapphire by metal-organic CVD (MOCVD). Both materials were sequentially transferred on Si/SiO_2 chips, resulting in a structure in which MoS_2 is on top of graphene (see Fig. 1g,h). Raman measurements were performed on the heterostructure as well as on pure graphene and

* Corresponding authors at: RWTH Aachen University, 52074 Aachen, Germany.
E-mail addresses: alwin.daus@imtek.uni-freiburg.de (A. Daus), max.lemme@eld.rwth-aachen.de (M.C. Lemme).

https://doi.org/10.1016/j.mne.2024.100256
Received 16 February 2024; Received in revised form 15 April 2024; Accepted 26 April 2024
Available online 28 April 2024

MoS_2 (see Fig. 2a). These locations were created by a defined misalignment of the materials.

2.1. Fabrication

CVD graphene on copper was prepared for transfer by spinning polymethyl methacrylate (PMMA) onto the graphene at 3000 rpm for 60 s and baking for 10 min at 120 °C. The copper substrate was removed by an etching solution of HCl and H_2O_2, and the graphene/PMMA stack was then rinsed in deionized water (DI water). Next, the graphene/PMMA stack was wet transferred onto Si chips covered with 90 nm of SiO_2 by placing the 2D material onto a drop of DI-water, which dried slowly, leaving the 2D material on the surface (Fig. 1a). After the graphene transfer, the PMMA was removed using acetone (Fig. 1b). Next, the samples were annealed at 300 °C for 10 min in vacuum (<1 mbar) (Fig. 1c). This step aided in the removal of PMMA residues [14] . With an AFM scan (Fig. S1) we cannot exclude residuals of PMMA, but the average coverage is sufficiently low to measure the Graphene/MoS_2 interaction with the Raman spectrometer with a spot size of about 300 nm without the PMMA influence. Raman control measurements taken before and after annealing showed no significant change in the spectrum of the graphene (Fig. S2 & S3). In analogy, MoS_2 on sapphire was coated with PMMA first. Then, the MoS_2/PMMA stack was delaminated from the sapphire using DI water and some force. Then the stack was transferred onto the graphene using another wet transfer process (Fig. 1d). The PMMA was dissolved in acetone, in the same way as from the graphene (Fig. 1e). A second annealing process for 1 h at 300 °C in vacuum (<1 mbar) finalized the sample fabrication. Raman scans were measured in areas with graphene, MoS_2, and their heterostructure before and after the last annealing process to analyze the materials separately and as a heterostructure, and to detect possible changes due to annealing (see Fig. 2 & S4). The entire fabrication process of the graphene-MoS_2 heterostructures is summarized in Fig. 1.

2.2. Raman spectroscopy

Raman area scans of the samples were performed to evaluate the interaction of the materials. We used a WiTec alpha300 R Raman imaging Microscope system with a 532 nm laser at 1 mW (about 14147 $\mu W/\mu m^2$) with a 300 g/mm grating, giving a resolution of 2.2 cm^{-1} and a range of 4100 rel. cm^{-1}. The full width at half maximum (FWHM) and the position of the Raman peaks, determined by Lorentzian fits [12,15,16], are typically the most important parameters. The Raman spectra were therefore analyzed for the graphene G and 2D peaks and the MoS_2 E^1_{2g} and A_{1g} peaks.

The Raman spectra of single-layer graphene (SLG) and bilayer graphene (BLG) differ in two aspects: firstly, the position of the 2D peak shifts towards higher wavenumbers (so-called blue shift) according to the number of layers [12,17]. Second, the FWHM of the 2D peaks for BLG is approximately twice that of SLG [15]. The positions of the E^1_{2g} and A_{1g} peaks in MoS_2 also differ depending on the number of layers present [18]. Finally, the Raman spectra are also altered when assembling MoS_2 and graphene into heterostructures [11,13]. In particular, the 2D peak position of graphene shifts comparably to that of 2 layers of graphene [11,13]. Theoretically, the positions of the MoS_2 peaks are also expected to shift in a similar way to the case of an additional MoS_2 layer, with the E^1_{2g} peak position decreasing and the A_{1g} peak position increasing [11,13]. However, this effect is less pronounced in our study because we used multilayer MoS_2 for which this effect is less prominent [18] and cannot be resolved by our Raman system with a Raman shift resolution of 2.2 cm^{-1}.

3. Results

The graphene remained stable after undergoing the annealing processes, as shown in Fig. 2, S2, S3 & S4. The only noticeable change was a reduction in the FWHM of the G-peak after the second annealing, indicating a decrease in internal material stress [19].

Fig. 2a shows spectra of single-layer graphene (SLG), bilayer graphene (BLG), and the heterostructure (Het). We observe a shift of the 2D peak to higher wavenumbers (blue shift) for bilayer graphene and the heterostructure, but no shift of the G peak. Fig. 2b shows an optical image of the sample, with the red frame indicating the measured area. The data were fitted using a Lorentzian function to determine the peak

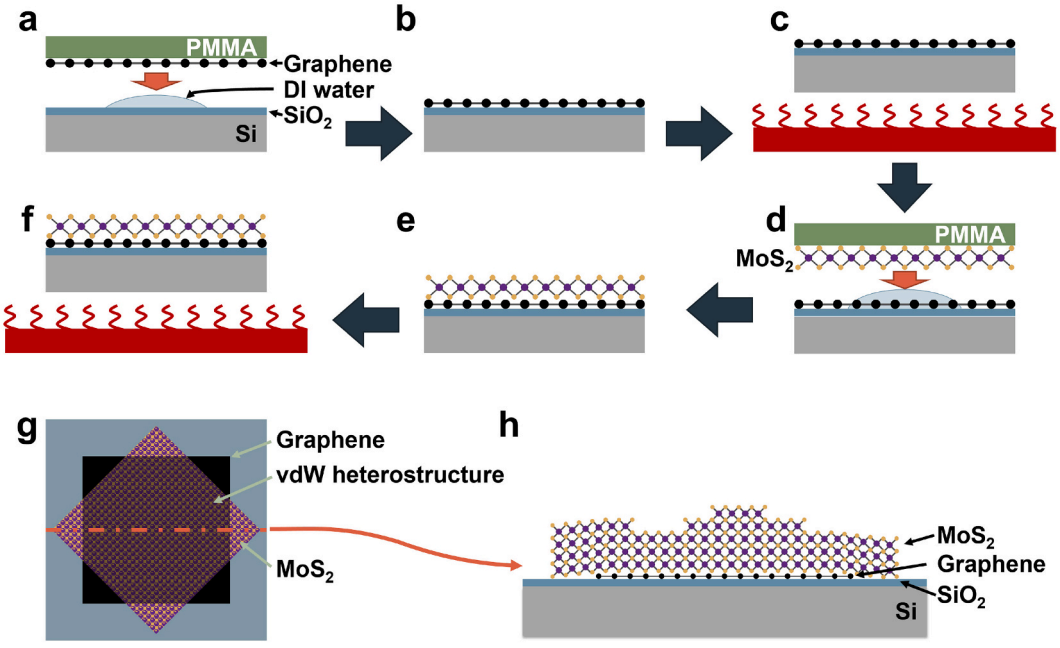

Fig. 1. Fabrication process of the heterostructures: a Graphene with a mechanical support polymer layer (PMMA 950 k A6) is wet transferred onto Si/SiO_2. b After PMMA removal. c Annealing of the Chip at 180 °C for 10 min. d Wet transfer of multilayer MoS_2, also supported by PMMA 950 k A6. e Removal of the PMMA. Raman measurements 'before annealing' were performed here. f Annealing of the heterostructure and Raman measurements 'after annealing'. g Top view of the final chip with a misalignment between the Graphene and the MoS_2. h Sideview of the sample along the cut line in g.

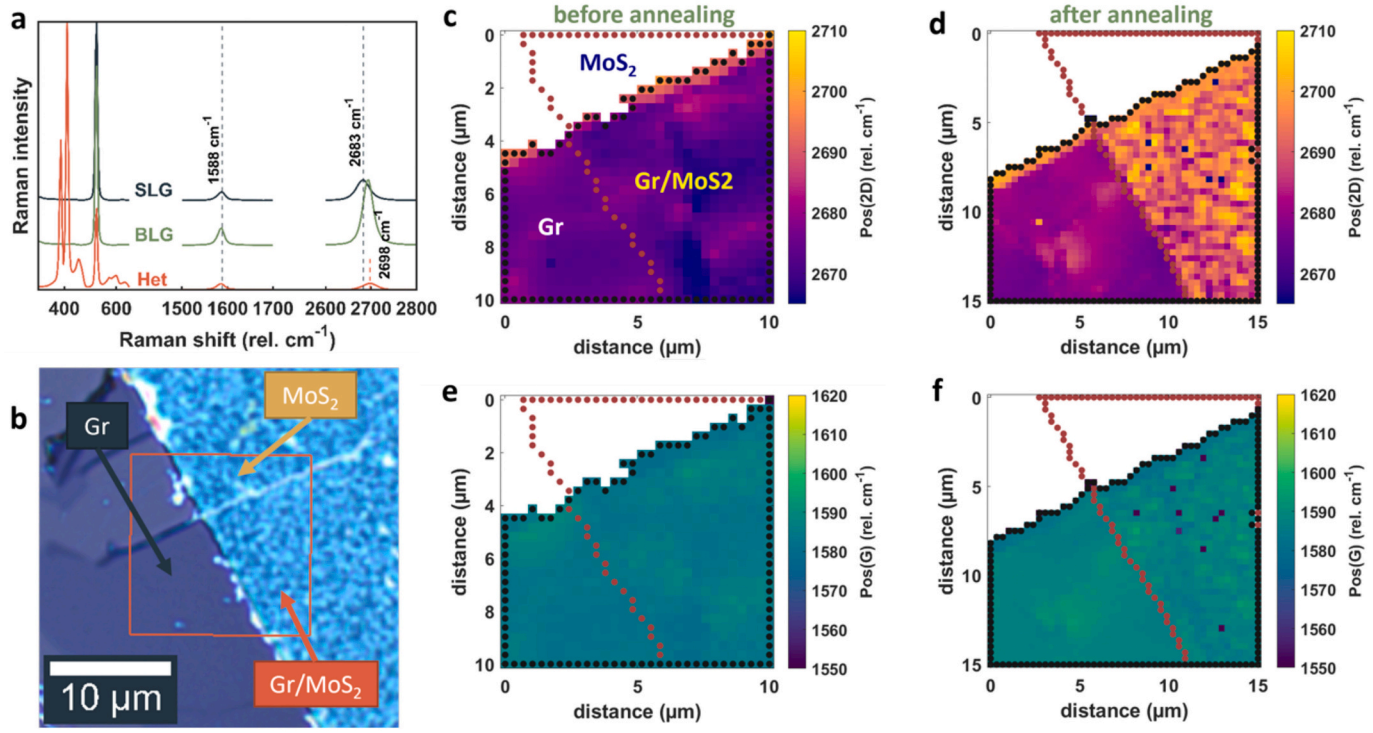

Fig. 2. a Raman spectrum of exemplary spots on single layer graphene (SLG), a bilayer graphene (BLG) and a heterostructure (Het). b Microscope image of the measured area (highlighted by the red frame). c-f: Position of the G and 2D peaks as an area scan. Black and red frame indicate graphene and MoS2 locations, respectively. The measured points are spaced 333 nm apart and are each approximately 300 nm in size. c,d 2D peak positions before and after annealing. e,f G peak positions before and after annealing. (For interpretation of the references to color in this figure legend, the reader is referred to the web version of this article.)

positions for every measurement within the frame. These results are shown in Fig. 2c-f. Here, c and d represent the position of the graphene 2D peak, while Fig. 2e and f represent the G peak. In addition, the Figures show the measurements before (c,e) and after (d,f) the second annealing process. MoS_2 was detected in areas surrounded by red dots, while black dots indicate the presence of graphene.

The graphene 2D peak measurements indicate a noticeable difference between the pre-annealing (Fig. 2c) and post-annealing (Fig. 2d) measurements. After annealing, there is a clear shift towards higher wavenumbers (blue shift) when comparing the pure graphene and the heterostructure. This shift was not observable before annealing (Fig. 2c). It indicates a change in the interaction between MoS_2 and graphene due to annealing, with the shifted 2D peak position pointing to a closely coupled heterostructure [11]. The graphene G peak does not shift, either before (Fig. 2e) or after (Fig. 2f) annealing, or between graphene and the heterostructure.

The temperatures and durations of the second annealing process were varied between 5 and 120 min and between 100 and 400 °C to investigate the effect of these variables on the quality of the heterostructure. The results of 17 experiments indicate that within the

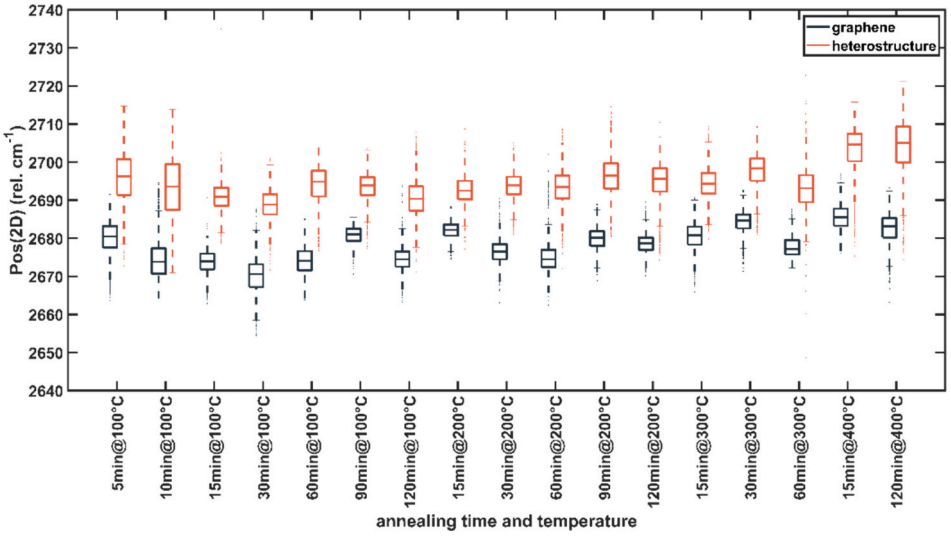

Fig. 3. Boxplot diagram showing variations in temperature and annealing duration. Dark blue boxes indicate the positions of the 2D peak in regions where graphene was solely measured. Conversely, red boxes indicate the positions of the graphene 2D peak in areas where heterostructures were measured. (For interpretation of the references to color in this figure legend, the reader is referred to the web version of this article.)

parameter window, these parameters do not have a significant effect on the position of the graphene 2D peak and, hence, do not appear to influence the quality of the heterostructure (see Fig. 3). In all cases, close coupling has been achieved.

Statistical analysis was performed on the difference between the graphene G and 2D peaks based on multiple measurements, as shown in Fig. 2. They enabled us to establish a threshold for close coupling between MoS_2 and graphene, above which a close-coupled heterostructure is formed. Peak positions from all Raman measurements were plotted in histograms (Fig. 4). The measurements were categorized as either graphene (dark blue) or heterostructure (red). The difference Δ between the positions of the graphene G and 2D peaks, referred to as "Pos(2D)-Pos (G)" was analyzed to identify any shifts. Fig. 4a shows the difference as a histogram for all measurement points, again labeled as either graphene or heterostructure. Additionally, Gaussian distributions were fitted to the bars, and their intersection was calculated, resulting in a threshold at a Δ Pos(2D)-Pos(G) of approximately 1100 cm^{-1}. Some overlap of the histograms is still visible, particularly for the heterostructure. This can be attributed to incomplete heterostructure formation in parts of the measurement areas, at which either residues are trapped between the transferred layers [14,20] or corrugations of 2D materials [21,22] result in insufficient coupling. In addition, a few bilayers are visible, shown in the part classified as graphene (dark blue bars) at about 1112 cm^{-1}. Nevertheless, the distinction between the two structures is still clearly visible. Employing this technique enables statistics-based differentiation of the heterostructure from the case of two 2D materials loosely placed on each other.

The 2D peak shift alone cannot be used to distinguish between a heterostructure and BLG, as both produce a similar shift [11] (Fig. 2a and Fig. 4a). Therefore, we turned our attention to the histograms of the FWHM of the graphene 2D peaks (Fig. 4b), which is an additional indicator to distinguish between heterostructures and BLG. The FWHM of SLG [15] and that of the heterostructure [11] are essentially the same, but BLG has a FWHM that is about twice as large, allowing us to distinguish between BLG and a heterostructure.

The process shown in Fig. 1 was also used to fabricate larger heterostructures using MoS_2 and graphene samples of approximately 1 × 1 cm^2, resulting in a heterostructure of approximately 48 mm^2 (Fig. 5a). A Raman scan was conducted on the sample with a measurement interval of 200 µm using a grating of 300 g/mm. Note that the size of a single measurement is much smaller than the distance between the measurements, i.e. the image is composed of individual measurements rather than a continuous area scan. Fig. 5b-d shows the results of the Raman measurements, with black dots surrounding the graphene area and red dots surrounding the MoS_2 area. Fig. 5b maps the position of the 2D peak, which was determined using a Lorentz approximation. Fig. 5c shows the difference $\Delta_{2D\text{-}G}$ in cm^{-1} between the positions of the G and 2D peaks. Both figures display the peak shift between the graphene and the heterostructure. Fig. 5d was created using the previously determined threshold value of 1100 cm^{-1} (Fig. 4a) to classify whether a coupled heterostructure is present. The resulting binary image shows areas with a $\Delta_{2D\text{-}G}$ >1100 cm^{-1} in green, while the areas with a $\Delta_{2D\text{-}G}$ <1100 cm^{-1} are colored red. Outside the MoS_2 region, the measurements with a $\Delta_{2D\text{-}G}$ >1100 cm^{-1} indicate BLG. Furthermore, it is evident that the formation of closely coupled heterostructures was unsuccessful in certain areas. Therefore, when attempting to fabricate large 2D heterostructures, it is crucial to always verify the coupling of the materials over the whole surface or device.

4. Conclusion

In this study, we have performed a thorough investigation of the interlayer coupling in graphene-MoS_2 heterostructures from large-scale, (MO)CVD 2D films. Our Raman spectroscopy data demonstrate the ability to quantitatively evaluate the coupling interaction between graphene and MoS_2, even for larger heterostructures at the mm^2 scale. The Raman analysis revealed significant shifts in the graphene peak separation, suggesting changes in the coupling behavior. By defining a threshold based on the graphene peak positions and analyzing the FWHM of the 2D peak, we statistically discriminate between regions of coupled heterostructures, bilayer graphene, and uncoupled stacked 2D materials. Annealing supports the formation of closely coupled heterostructures, although different annealing parameters did not significantly affect the results. Furthermore, the study extends the analysis to larger scale heterostructures, demonstrating the suitability of the proposed Raman-based methodology for industrial implementation. The data obtained from mm^2-scale heterostructures revealed areas of insufficient coupling. This indicates that the typical wet transfer technique employed here to assemble heterostructures needs further improvement. The proposed non-destructive Raman spectroscopy approach is a suitable tool to further optimize 2D material transfer and to evaluate the close coupling in 2D material heterostructures on a large scale.

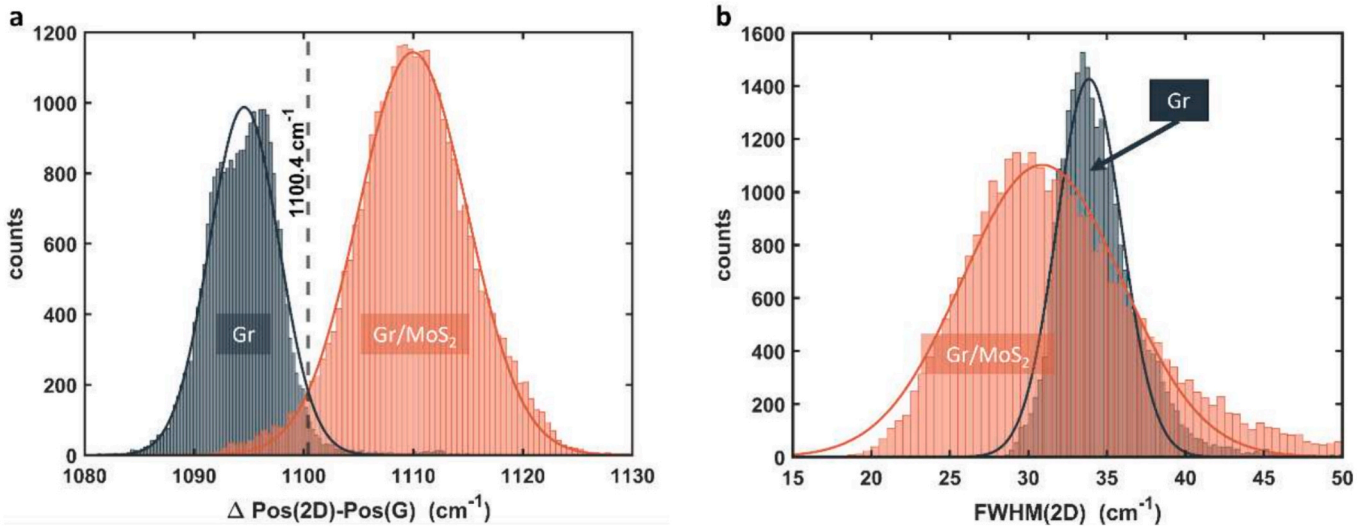

Fig. 4. a Histogram of the difference (Δ) in peak position (Pos) for 2D and G peaks for the area in Fig. 2, with Gaussian distribution fits and determination of their intersection. b Histogram of the FWHM(2D). Red and dark blue indicate the heterostructures (het) and bare graphene (gr), respectively. (For interpretation of the references to color in this figure legend, the reader is referred to the web version of this article.)

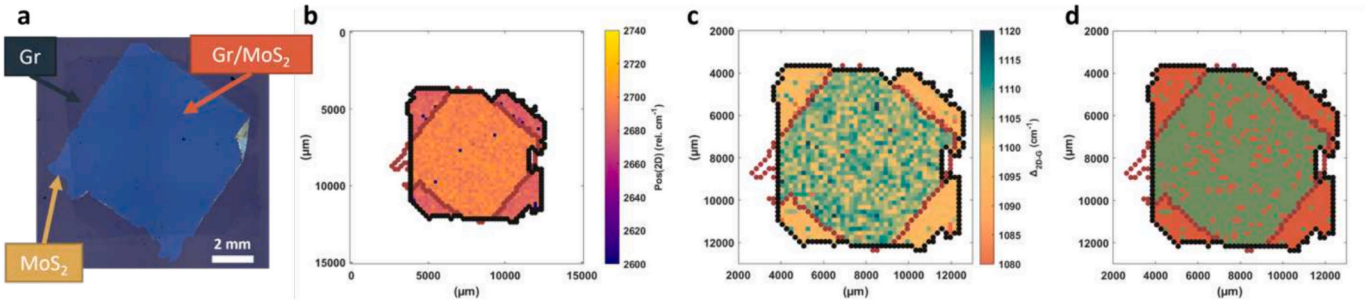

Fig. 5. Large-area Raman measurement of a square millimeter scale fabricated heterostructure: a Optical image of the measured area with a size of approx. 48 mm^2. b-d Black and red frame indicate graphene and MoS_2 locations. b Graphene 2D peak positions of the whole structure. c Difference ($\Delta_{2D\text{-}G}$) between the graphene G and 2D peak positions. d Binary division of the data of c with values >1100 cm^{-1} in green and the rest in red. (For interpretation of the references to color in this figure legend, the reader is referred to the web version of this article.)

Declaration of competing interest

The authors declare that they have no known competing financial interests or personal relationships that could have appeared to influence the work reported in this paper.

Data availability

Data will be made available on request.

Acknowledgement

This work was financially supported by the German Research Foundation (DFG) under the projects 2D-NEMS (LE 2440/11-1), (VE 597/5-2) and the Emmy Noether Programme (506140715), as well as by the German Federal Ministry of Education and Research (BMBF) under the projects nanodiag BW (03ZU1208xx), NeuroSys (03ZU1106xx) and NEUROTEC (16ME0399 & 16ME0400).

Appendix A. Supplementary data

Supplementary data to this article can be found online at https://doi.org/10.1016/j.mne.2024.100256.

References

[1] C.-J. Shih, Q.H. Wang, Y. Son, Z. Jin, D. Blankschtein, M.S. Strano, Tuning on-off current ratio and field-effect mobility in a MoS(2)-graphene heterostructure via Schottky barrier modulation, ACS Nano 8 (2014) 5790–5798, https://doi.org/10.1021/nn500676t.

[2] W. Zhang, C.-P. Chuu, J.-K. Huang, C.-H. Chen, M.-L. Tsai, Y.-H. Chang, C.-T. Liang, Y.-Z. Chen, Y.-L. Chueh, J.-H. He, M.-Y. Chou, L.-J. Li, Ultrahigh-gain photodetectors based on atomically thin graphene-MoS2 heterostructures, Sci. Rep. 4 (2014) 3826, https://doi.org/10.1038/srep03826.

[3] M.C. Lemme, S. Wagner, K. Lee, X. Fan, G.J. Verbiest, S. Wittmann, S. Lukas, R. J. Dolleman, F. Niklaus, H.S.J. van der Zant, G.S. Duesberg, P.G. Steeneken, Nanoelectromechanical sensors based on suspended 2D materials, Research 2020 (2020) 8748602, https://doi.org/10.34133/2020/8748602.

[4] E.M. Alexeev, A. Catanzaro, O.V. Skrypka, P.K. Nayak, S. Ahn, S. Pak, J. Lee, J. I. Sohn, K.S. Novoselov, H.S. Shin, A.I. Tartakovskii, Imaging of interlayer coupling in van der Waals Heterostructures using a bright-field optical microscope, Nano Lett. 17 (2017) 5342–5349, https://doi.org/10.1021/acs.nanolett.7b01763.

[5] H. Terrones, F. López-Urías, M. Terrones, Novel hetero-layered materials with tunable direct band gaps by sandwiching different metal disulfides and diselenides, Sci. Rep. 3 (2013) 1549, https://doi.org/10.1038/srep01549.

[6] A. Ebnonnasir, B. Narayanan, S. Kodambaka, C.V. Ciobanu, Tunable MoS 2 bandgap in MoS 2 -graphene heterostructures, Appl. Phys. Lett. 105 (2014) 031603, https://doi.org/10.1063/1.4891430.

[7] G. Giovannetti, P.A. Khomyakov, G. Brocks, P.J. Kelly, J. Van Den Brink, Substrate-induced band gap in graphene on hexagonal boron nitride: *ab initio* density functional calculations, Phys. Rev. B 76 (2007) 073103, https://doi.org/10.1103/PhysRevB.76.073103.

[8] H. Coy Diaz, J. Avila, C. Chen, R. Addou, M.C. Asensio, M. Batzill, Direct observation of interlayer hybridization and Dirac relativistic carriers in graphene/MoS 2 van der Waals Heterostructures, Nano Lett. 15 (2015) 1135–1140, https://doi.org/10.1021/nl504167y.

[9] D. Pierucci, H. Henck, J. Avila, A. Balan, C.H. Naylor, G. Patriarche, Y.J. Dappe, M. G. Silly, F. Sirotti, A.T.C. Johnson, M.C. Asensio, A. Ouerghi, Band alignment and Minigaps in monolayer MoS 2 -graphene van der Waals Heterostructures, Nano Lett. 16 (2016) 4054–4061, https://doi.org/10.1021/acs.nanolett.6b00609.

[10] L. Britnell, R.V. Gorbachev, R. Jalil, B.D. Belle, F. Schedin, A. Mishchenko, T. Georgiou, M.I. Katsnelson, L. Eaves, S.V. Morozov, N.M.R. Peres, J. Leist, A. K. Geim, K.S. Novoselov, L.A. Ponomarenko, Field-effect tunneling transistor based on vertical graphene Heterostructures, Science 335 (2012) 947–950, https://doi.org/10.1126/science.1218461.

[11] K.-G. Zhou, F. Withers, Y. Cao, S. Hu, G. Yu, C. Casiraghi, Raman modes of MoS 2 used as fingerprint of van der Waals interactions in 2-D crystal-based Heterostructures, ACS Nano 8 (2014) 9914–9924, https://doi.org/10.1021/nn5042703.

[12] A. Jorio, Raman spectroscopy in graphene-based systems: prototypes for nanoscience and Nanometrology, ISRN Nanotechnology 2012 (2012) 1–16, https://doi.org/10.5402/2012/234216.

[13] M. Yang, L. Wang, G. Hu, X. Chen, P.L. Gong, X. Cong, Y. Liu, Y. Yang, X. Li, X. Zhao, X. Liu, Optical identification of interlayer coupling of graphene/MoS2 van der Waals heterostructures, Nano Res. 14 (2021) 2241–2246, https://doi.org/10.1007/s12274-020-3215-9.

[14] B. Zhuang, S. Li, S. Li, J. Yin, Ways to eliminate PMMA residues on graphene —— superclean graphene, Carbon 173 (2021) 609–636, https://doi.org/10.1016/j.carbon.2020.11.047.

[15] A.C. Ferrari, D.M. Basko, Raman spectroscopy as a versatile tool for studying the properties of graphene, Nat. Nanotechnol. 8 (2013) 235–246, https://doi.org/10.1038/NNANO.2013.46.

[16] A. Das, S. Pisana, B. Chakraborty, S. Piscanec, S.K. Saha, U.V. Waghmare, K. S. Novoselov, H.R. Krishnamurthy, A.K. Geim, A.C. Ferrari, A.K. Sood, Monitoring dopants by Raman scattering in an electrochemically top-gated graphene transistor, Nat. Nanotechnol. 3 (2008) 210–215, https://doi.org/10.1038/nnano.2008.67.

[17] R. Saito, M. Hofmann, G. Dresselhaus, A. Jorio, M.S. Dresselhaus, Raman spectroscopy of graphene and carbon nanotubes, Adv. Phys. 60 (2011) 413–550, https://doi.org/10.1080/00018732.2011.582251.

[18] H. Li, Q. Zhang, C.C.R. Yap, B.K. Tay, T.H.T. Edwin, A. Olivier, D. Baillargeat, From bulk to monolayer MoS2: evolution of Raman scattering, Adv. Funct. Mater. 22 (2012) 1385–1390, https://doi.org/10.1002/adfm.201102111.

[19] T.M.G. Mohiuddin, A. Lombardo, R.R. Nair, A. Bonetti, G. Savini, R. Jalil, N. Bonini, D.M. Basko, C. Galiotis, N. Marzari, K.S. Novoselov, A.K. Geim, A. C. Ferrari, Uniaxial strain in graphene by Raman spectroscopy: G peak splitting, Grüneisen parameters, and sample orientation, Phys. Rev. B 79 (2009), https://doi.org/10.1103/PhysRevB.79.205433.

[20] D. Braun, M.D. Ganeriwala, L. Völkel, K. Ran, S. Lukas, E.G. Marín, O. Hartwig, M. Prechtl, T. Wahlbrink, J. Mayer, G.S. Duesberg, A. Godoy, A. Daus, M. C. Lemme, Non-Volatile Resistive Switching of Polymer Residues in 2D Material Memristors, 2023, https://doi.org/10.48550/arXiv.2309.13900.

[21] V. Geringer, M. Liebmann, T. Echtermeyer, S. Runte, M. Schmidt, R. Ruckamp, M. C. Lemme, M. Morgenstern, Intrinsic and extrinsic corrugation of monolayer graphene deposited on SiO2, Phys. Rev. Lett. 102 (2009) 076102–076104.

[22] Z. Cheng, H. Zhang, S.T. Le, H. Abuzaid, G. Li, L. Cao, A.V. Davydov, A.D. Franklin, C.A. Richter, Are 2D interfaces really flat? ACS Nano 16 (2022) 5316–5324, https://doi.org/10.1021/acsnano.1c11493.